Ion Response to Relativistic Electron Bunches in the Blowout Regime of Laser-Plasma Accelerators

K. I. Popov,[1] W. Rozmus,[1] V. Yu. Bychenkov,[1,2] N. Naseri,[1] C. E. Capjack,[3] and A. V. Brantov[2]
[1]*Theoretical Physics Institute, University of Alberta, Edmonton T6G 2J1, Alberta, Canada*
[2]*P. N. Lebedev Physics Institute, Russian Academy of Sciences, Moscow 119991, Russia*
[3]*Department of Electrical Computer, Engineering, University of Alberta, Edmonton T6G 2J1, Alberta, Canada*
(Received 9 March 2010; published 1 November 2010)

The ion response to relativistic electron bunches in the so called bubble or blowout regime of a laser-plasma accelerator is discussed. In response to the strong fields of the accelerated electrons the ions form a central filament along the laser axis that can be compressed to densities 2 orders of magnitude higher than the initial particle density. A theory of the filament formation and a model of ion self-compression are proposed. It is also shown that in the case of a sharp rear plasma-vacuum interface the ions can be accelerated by a combination of three basic mechanisms. The long time ion evolution that results from the strong electrostatic fields of an electron bunch provides a unique diagnostic of laser-plasma accelerators.

DOI: 10.1103/PhysRevLett.105.195002 PACS numbers: 52.38.Hb, 52.38.Kd

The interaction of ultrashort relativistic laser pulses with underdense plasma can serve as a source of accelerated electrons and ions [1–8]. The development of laser-plasma accelerators (LPAs) was dramatically transformed in 2004 when three groups [1–3] produced high-quality electron bunches characterized by a large charge, a high mean energy with small spread and a low divergence. In these experiments electrons were accelerated in the blowout, or so called ''bubble'' regime of the LPA [4], where the laser intensity is so high that electrons are expelled from the region close to the laser axis and an ion cavity is formed which also encloses the laser pulse. In addition to fully expelled particles, some of the plasma electrons are self-injected into the ion cavity where they form a dense bunch and can be accelerated to high energies. In this Letter, we will focus on the long time plasma evolution that follows the electron acceleration and includes the formation and expansion of the central ion filament, and ion acceleration in the forward and transverse directions. Simulations of short high intensity laser pulse interactions [9] have shown that the ions form a dense filament along the laser axis in an evacuated channel. Its formation was explained by the ''inverted corona'' effect [10] wherein the hot plasma collapses on the axis from the channel walls. Ponderomotive effects rather than plasma wall heating have been employed recently [11] to describe the ion convergence towards the center on the long time scale. We have found that an ion filament in the blowout regime of LPAs is formed due to the strong electrostatic field of the trapped electron bunch. The transverse field of the relativistic electron bunch provides an initial impulse for the background ions from within the central region of the bubble. The radius of this region is approximately equal to that of the electron beam and contains ions that could later be compressed by 2 orders of magnitude and higher, in the axial filament. The formation of the central filament occurs simultaneously with the expulsion of the outer ions from the cavity towards its edge. The compressed central ion filament contains a strongly unbalanced ion charge that subsequently leads to ion expansion in the radial direction. However, at the rear plasma-vacuum boundary, the collimated high density ion beam also generates a strong longitudinal field which contributes to ion acceleration. On a long time scale, the expansion of the central filament and of the formed plasma channel contributes to ion acceleration and to density structures observed in experiments [12] that could provide a useful diagnostic for the accelerated electron bunch.

Central to our work are 3D particle-in-cell (PIC) simulations with the electromagnetic relativistic code SCPIC [13]. We will discuss our results by taking as an example simulations where the following parameters are used: the laser is linearly polarized in the XY plane and has a maximum intensity equal to 10^{22} W/cm^2 and is focused to a 5 wavelength FWHM spot size. The laser wavelength is equal to $\lambda = 1$ μm, and the pulse duration is equal to 10 fs (FWHM). These are parameters consistent with the bubble regime scaling [14] at the relatively high plasma density $n \sim 0.1 n_{cr}$, where n_{cr} is the electron critical density. We have chosen this high background plasma density in order to generate a very fast ion response to the transverse field of the electron bunch which could have a density up to $10 n_{cr}$. However as long as the laser interacts with a plasma in the blowout regime, the plasma demonstrates a universal long time response that includes central filament formation. Later on we will also describe such a response for the parameters of one of the first successful acceleration experiments in the blowout regime [1]. The electron-to-ion mass ratio in our simulations is $1/1836$ and ion $Z = 1$. We have used $9 \times 14 \times 14$ points per λ^3 and 8 particles of each species per cell in the simulations.

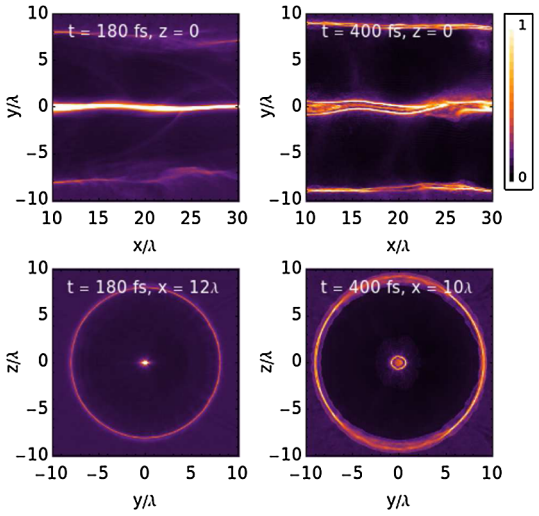

FIG. 1 (color online). Ion particle density, normalized by the electron critical density n_{cr}, behind the laser pulse. The maximum level is truncated by 1.

Figure 1 shows the ion density at two different moments in time after the laser pulse has passed. The patterns in Fig. 1 correspond to the plasma compression to a dense ion axial filament and its subsequent expansion in a form of a ringlike structure in the transverse cross section. The maximum particle density in the filament exceeds the initial density by more than 2 orders of magnitude. The filament forms behind the laser pulse in several tens of femtoseconds.

The propagation of the laser in the plasma results in the formation of a bubble as illustrated by the charge density distribution in Fig. 2(a). The electron charge density in Fig. 2(a) corresponds to a typical blowout regime interaction [4]. The self-injected relativistic electrons are confined in the transverse direction by their own magnetic field.

The long time ion evolution is the result of the transverse ion current distribution that is established in the plasma. This is shown in Fig. 2(b) at $t = 115$ fs. The ions within the region occupied by the electron bunch as seen in Fig. 2(a) are accelerated in the radial direction in the field of an electron bunch, move towards the axis and later form the central filament. The rest of the ions in the laser-formed cavity acquire initial velocities which result in their motion away from the central axis due to the repulsive forces between them.

Figure 3(a) shows the phase space $(y - p_y)$ of ions taken from the PIC simulations at $x = 15\lambda$ and $z = 0$ at $t = 115$ fs. The particles at $|y| \lesssim 3\lambda$ move towards the axis, and those at $|y| \gtrsim 3\lambda$ move outwards. Figure 3(b) shows a similar ion distribution in a phase space, $y - p_y$, from the PIC simulations for the parameters of the experiment in Ref. [1], i.e., for $I = 2.5 \times 10^{18}$ W/cm^2, 40 fs laser pulse with $\lambda = 0.8$ μm, focused into a 25 μm spot, interacting with a gas-jet plasma having particle density $n = 0.01 n_{cr}$. As in Fig. 3(a), the transverse ion momentum from Fig. 3(b) will determine plasma evolution in terms of the compression of the central part and the transverse expansion of the outer region as we will discuss below. In this example the initial ion velocities are much lower and therefore the subsequent plasma evolution will take a much longer time. It is important, however, that it will involve the similar stages of the filament formation and its subsequent explosion.

In order to discuss the long time plasma evolution, we first note the high kinetic energy of electrons behind the bubble. Therefore we will assume below that these hot electrons form a uniform background for ion evolution. The most conservative estimate of the ion compression ratio can be made if the background electron charge that partially neutralizes the compressing dense filament is ignored altogether. We use this assumption in the estimation and approximate the momenta $p_y(y)$ of ions located at $|y| \lesssim 0.8\lambda$ [the area shown by the two vertical lines in Fig. 3(a)], by a linear function $p_y = -\alpha y$. It can be shown that trajectories of ions that originate on this line do not cross, at least not before the maximum compression stage is reached. Thus, particles move in the field equal to the field of a thin wire located along the laser axis: $E_r(r, t) = 2r(t)\Delta Q/\Delta z = 2\pi r_0^2 e n_0 / r(t)$, where $r(t)$ is the transverse position of ion at time t, $r_0 = r(0)$, en_0 is initial charge density of ions, and ΔQ is the charge inside the cylinder formed by the accelerated electron bunch of height Δz and radius r_0 at $t = 0$. The maximum compression ratio can be calculated by using energy conservation: $M v_0^2/2 = -e[\phi(R) - \phi(R_s)] = 2e^2 n_0 \pi r_0^2 \ln(R/R_s)$, where R_s is the stopping location of the particle starting inward motion

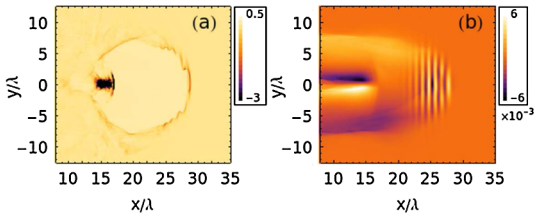

FIG. 2 (color online). A snapshot at $t = 115$ fs in the plane XY passing through the axis of the channel: (a) the normalized charge density ρ/en_{cr} (minimum level is set to -3); (b) the normalized transverse ion current density $J_{tr}/en_{cr}c$.

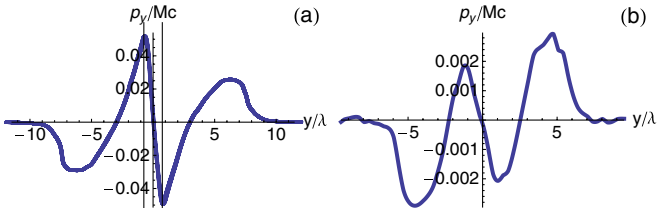

FIG. 3 (color online). The transverse phase space $y - p_y$ of ions from PIC simulations at $x = 15\lambda$ and $z = 0$ at $t = 115$ fs; (b) a similar phase space plot from the PIC simulations with parameters from Ref. [1].

at $r = R$, v_0 is the initial velocity of an ion and M is its mass. The compression ratio C_R of the collapsed ion wire is

$$C_R = \left(\frac{R}{R_s}\right)^2 = \exp\left(2\frac{v_0^2}{\omega_L^2 R^2}\right). \quad (1)$$

For the parameters considered in our first example ($n_0 = 0.1 n_{cr}$, $R \approx 0.8\lambda$, $v_0 \approx 0.05c$) from Fig. 3(a), Eq. (1) results in $C_R \approx \exp(3.6) \approx 40$, which is comparable to the PIC simulation results.

An electrostatic 1D cylindrically symmetric gridless large particle code has been developed to study the long time ion evolution and in order to examine the viability of such results as a diagnostic of bubble electron acceleration. In this code, the macroparticles are represented by hollow charged cylinders with the given q/m ratio. The cylinders move in the self-consistent field obtained from the Gauss theorem. The phase space distributions of the ions from Figs. 3(a) and 3(b) are used as initial conditions in the simulations. The results of simulations with this code are shown in Fig. 4.

At $t = t_0 = 0$, we start with a homogeneous and neutral plasma. In the two examples ions have a negative velocity at $t = 0$ and thus move first inward [Figs. 4(a) and 4(c)]. This leads to the buildup of ion charge near $r = 0$ and gives rise to a repulsive electrostatic force. At $t = t_1$ when the compression is maximum this force stops the contraction of particles near $r = 0$. The moment of the maximum compression stage in Figs. 4(a) and 4(b) is consistent with results of our 3D PIC simulations. Note the very different time scales, $t_1 = 44$ fs in Fig. 4(b) and $t_1 = 300$ fs in Fig. 4(d), and also the dramatically different compression ratios at these times for our two examples. Clearly the relatively small number of accelerated electrons in the experiment of Ref. [1] has triggered a modest ion response as compared to strong response in our PIC simulations corresponding to Fig. 1. Also due to the exponential dependence in Eq. (1) the compression ratio is very sensitive to the laser parameters and can reach more than 4 orders of magnitude in our cylindrically symmetric model [Fig. 4(b)]. For longer times, $t > t_1$, the compressed filament explodes in the radial direction. The electrostatic field in the maximum compression stage is zero on the axis and has a local maximum at $r > 0$. Upon the start of the explosion stage, the particles near this local maximum acquire a higher outward velocity than their neighbors. This leads to alignment of the faster particles with their slower neighbors in phase space and the formation of a collisionless shock [curves at $t = t_2$ in Figs. 4(a) and 4(b)]. Later on, the faster ions outrun the slower ones, and the shock splits into two (cf. [15]). Similar processes take place at the large radius [$r \approx 8\lambda$ in Figs. 1 and 3(a)], where outward ion motion is accompanied by multiflows in the phase space and shock formation.

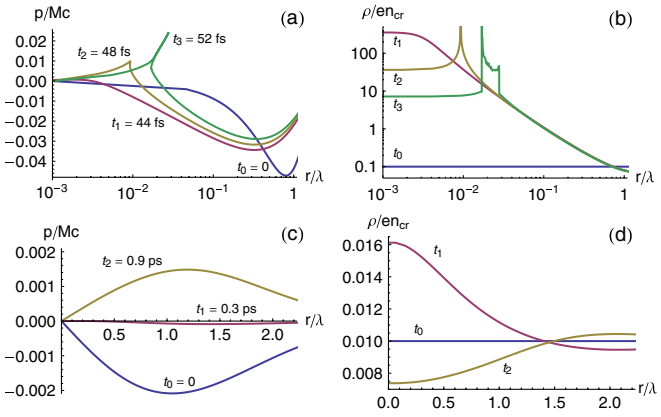

FIG. 4 (color online). Formation and explosion of the dense ion filament in the 1D cylindrically symmetric electrostatic model: (a) ions in the phase space; (b) ion particle density. (c), (d) Ion phase space and particle density evolutions for the parameters of Ref. [1].

The electrostatic cylindrical code can produce density profiles as in Figs. 4(b) and 4(d) at late times, unavailable for 3D PIC simulations, when these profiles will be relevant for the comparison with experimental interferometric and shadowgraphy measurements. For the parameters of our first example, Fig. 1, we note that the shocks from Fig. 4(b) were not well resolved by the spatial grid in the 3D simulations. However, the density increase between the shocks can be seen in Fig. 1 at later time as a ring structure. The finite electron temperature leads to an accumulation of slower electrons and results in an ion density increase near $r = 0$ in Fig. 1 (cf. [16]). The shocks have not formed in the simulations with parameters of Ref. [1] [Figs. 4(c) and 4(d)] due to the much smaller density and field gradients. The faster particles cannot outrun their slower neighbors because the latter are able to accelerate to comparable velocities. However, the expansion process is still accompanied by formation of a ringlike structure [Fig. 4(d)].

We now discuss the ion dynamics at the rear plasma-vacuum boundary. Our simulations have shown that in the case of a monotonically decaying plasma density at the boundary, the filament at the maximum compression stage has a smaller radius in the ramp than inside the plasma; i.e., it is sharpened. When a bunch of trapped electrons leaves the bulk of a plasma, it keeps moving, pulling the background ions towards it. As a result, the ions from the boundary acquire the same initial inward velocity v_0 as the ones from the bulk of plasma. However, the transverse repulsion between the ions is now smaller due to the decreased plasma density in the ramp. This leads to decreasing of ω_L in Eq. (1) and, as a result, to a stronger compression.

The following three mechanisms were found important for longitudinal ion acceleration in the bubble regime: (1) acceleration of ions at the boundary in the field of the positively charged laser-formed cavity; (2) acceleration by the transient field appearing during bubble destruction; and (3) Coulomb explosion of the self-compressed ion filament.

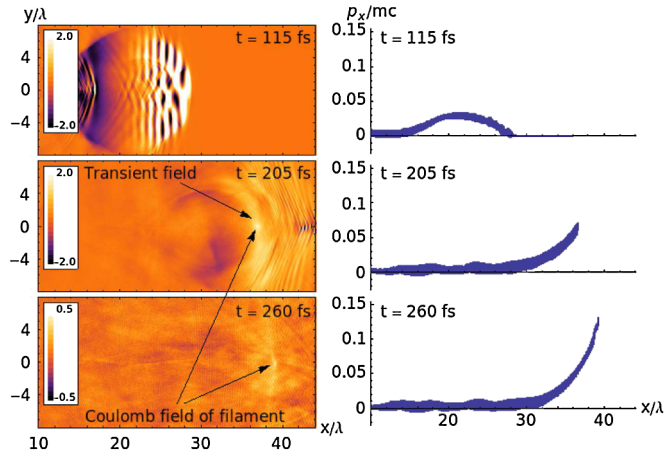

FIG. 5 (color online). Longitudinal electric field distribution in the XY plane passing through the laser axis (left column) and ions from the vicinity of the laser axis in the longitudinal phase space (right column) at different moments in time. The steplike plasma-vacuum interface is located at $x = 36\lambda$.

Different stages of acceleration are illustrated in Fig. 5. When the bubble propagates inside plasma, it accelerates ions to the right of its center and decelerates ions in the left part. The net acceleration of the ions in the longitudinal direction is zero. However, the ions located at the edge of the plasma never decelerate since the bubble is destroyed at the edge. These ions acquire a nonzero energy. This process could be also identified as a Coulomb explosion of the bubble (cf. [17]).

The moving cavity can be represented as an ion current in the longitudinal direction. When this current reaches the edge of the plasma, it stops. As a result, a transient electric field appears that tries to sustain the current and thus further accelerates the ions. This field is identified by an arrow in Fig. 5 at $t = 205$ fs. Under conditions of bubble acceleration the above mechanism dominates the "magnetic field annihilation" [5,8,17] that occurs in the expansion of a magnetized plasma into a vacuum.

At the next stage, the collapsed ion filament explodes. As was stated above, the filament has a net positive charge due to an incomplete neutralization by electrons. The resulting electrostatic field has a longitudinal component at the tip of the ion needle. This field is indicated by arrows in Fig. 5 at $t = 205$ fs and $t = 280$ fs and it results in the further acceleration of ions.

The net ion acceleration is a combination of the three processes described above. The efficiency of these acceleration mechanisms increases for a sharper plasma-vacuum interface. Therefore for an ion acceleration scheme, one could consider different target materials such as aerogels or foams [18] to increase plasma density and the density gradient at the boundary. Simulations with the given laser parameters for different plasma densities with a steplike interface have shown an approximately linear dependence (cf. [17]) for the maximum energy acquired by the ions for $t \to \infty$. The numerical fit gives the maximum ion energy $\epsilon_{\max} \approx 140 \frac{n}{n_{\rm cr}}$ MeV for underdense plasma, $n/n_{\rm cr} \in (0.1, 1)$, for laser parameters of Fig. 1.

In summary, we have studied ion behavior in the bubble regime of a laser-plasma accelerator. The formation of a central high density ion filament in response to the accelerated electron bunch and its subsequent long time evolution provides unique insight into the bubble acceleration process. Electrostatic simulations have shown that the filaments develop on a ~ps time scale and therefore are accessible to interferometric and shadowgraphy measurements [12]. The experimental detection of plasma filaments will enable identification of the history of a trapped electron bunch, including its trajectory and symmetry.

In addition to the possible diagnostic applications, the highly compressed ion filament has provided additional focusing of the electron bunch trapped in the second bubble in a simulation with two laser pulses propagating one after the other.

This work was partly supported by the Natural Sciences and Engineering Research Council of Canada and the Russian Foundation for Basic Research. One of the authors (K. I. P.) would like to acknowledge discussions and support from Dr. Lora Ramunno at the University of Ottawa where also a part of this work has been done.

[1] S. P. D. Mangles *et al.*, Nature (London) **431**, 535 (2004).
[2] C. G. R. Geddes *et al.*, Nature (London) **431**, 538 (2004).
[3] J. Faure *et al.*, Nature (London) **431**, 541 (2004).
[4] E. Esarey *et al.*, Rev. Mod. Phys. **81**, 1229 (2009).
[5] Y. Sentoku *et al.*, Phys. Rev. E **62**, 7271 (2000).
[6] M. S. Wei *et al.*, Phys. Rev. Lett. **93**, 155003 (2004).
[7] L. Willingale *et al.*, Phys. Rev. Lett. **96**, 245002 (2006).
[8] Y. Fukuda *et al.*, Phys. Rev. Lett. **103**, 165002 (2009).
[9] S. V. Bulanov *et al.*, JETP Lett. **71**, 407 (2000).
[10] G. A. Askar'yan *et al.*, Laser Part. Beams **18**, 335 (2000).
[11] A. Macchi *et al.*, Plasma Phys. Controlled Fusion **51**, 024005 (2009).
[12] Z. Najmudin *et al.*, Phys. Plasmas **10**, 438 (2003).
[13] K. I. Popov *et al.*, Phys. Plasmas **16**, 053106 (2009).
[14] S. Gordienko and A. Pukhov, Phys. Plasmas **12**, 043109 (2005).
[15] V. F. Kovalev *et al.*, Phys. Plasmas **14**, 053103 (2007).
[16] K. I. Popov *et al.*, Phys. Plasmas **17**, 083110 (2010).
[17] T. Zh. Esirkepov *et al.*, JETP Lett. **70**, 82 (1999).
[18] L. Willingale *et al.*, Phys. Rev. Lett. **102**, 125002 (2009).